

Differential Short-term Synaptic Plasticity and Transmission of Complex Spike Trains: to Depress or to Facilitate?

Victor Matveev^{1,2} and Xiao-Jing Wang¹

¹Volen Center for Complex Systems, Brandeis University, Waltham, MA 02454 and ²Mathematical Research Branch, NIDDK, National Institutes of Health, Bethesda, MD 20892, USA

Experimental studies have revealed conspicuous short-term facilitation and depression that are expressed differentially at distinct classes of cortical synapses. To explore computational implications of synaptic dynamics, we investigated transmission of complex spike trains through a stochastic model of cortical synapse endowed with short-term facilitation and vesicle depletion. Inputs to the synapse model were either real spike train data recorded from the visual and prefrontal cortices of behaving monkeys, or were generated numerically with prescribed temporal statistics. We tested the hypothesis that short-term facilitation could enable synapses to filter out single spikes and favor bursts of action potentials. We found that the ratio between release probabilities for a burst spike and an isolated spike grows monotonically with increasing number of spikes per burst, and with increasing interval between isolated spikes. Burst detection is optimal when the facilitation time constant matches the average burst duration. Using fractal-like spike patterns characterized by long-term power-law temporal correlations and similar to those seen in sensory neurons, we found that facilitation increases correlation at short time scales. In contrast, depression leads to a dramatic reduction in temporal correlations at all time scales, and to a flat ('whitened') power spectrum, thereby decorrelating natural input signals.

Introduction

Transient activity-dependent synaptic plasticity is a prevalent feature of both vertebrate and invertebrate neural systems, regulating synaptic efficacy at a variety of time scales, from milliseconds to minutes (Magleby, 1987; Zucker, 1989, 1996; Fisher *et al.*, 1997). Recently there has been a resurgence of interest in this topic, and a growing number of experimental results on cortical synapses (Stevens and Wang, 1995; Debanne *et al.*, 1996; Markram and Tsodyks, 1996; Thomson *et al.*, 1996; Abbott *et al.*, 1997; Buhl *et al.*, 1997; Dobrunz and Stevens, 1997; Castro-Alamancos and Connors, 1997; Thomson and Deuchars, 1997; Varela *et al.*, 1997, 1999; Ali *et al.*, 1998; Galarreta and Hestrin, 1998; Dittman *et al.*, 2000; Kreitzer and Regehr, 2000). Theoretical studies have shown that short-term depression can have dramatic effects on synaptic response to inputs of changing firing rates (Abbott *et al.*, 1997; Tsodyks and Markram, 1997), and it was also suggested that depression may be involved in generation of rhythmic activity in certain neural systems (Senn *et al.*, 1996; O'Donovan and Chub, 1997; O'Donovan and Rinzel, 1997). It was also proposed that short-term plasticity may underlie the selectivity of neurons for temporal patterns in afferent signals (Buonomano and Merzenich, 1995; Buonomano, 2000). These results highlighted the notion that synapses are readily modifiable and play an active role in the computation carried out by a neural circuit.

Short-term plasticity is differentially expressed at synapses, in a target-cell-specific manner. For example, intracellular recordings from neocortical slices revealed that afferents of a pyramidal cell innervating another pyramidal cell and an

interneuron display frequency-dependent depression and facilitation respectively (Thomson, 1997; Markram *et al.*, 1998; Varela *et al.*, 1999). In another study, synaptic responses evoked by a pyramidal cell in a bitufted interneuron showed facilitation, while the responses evoked by the same pyramidal cell in a multipolar interneuron exhibited short-term depression (Reyes *et al.*, 1998). Target-cell specific short-term plasticity of synapses of pyramidal cells was also observed in the hippocampus (Ali and Thomson, 1998). All these data raise the questions of why short-term plasticity should be synapse-specific, and when facilitation or depression is desirable from a computational point of view. To address these questions, we need to study the interplay between presynaptic firing patterns and synaptic dynamics, for example by using natural spike trains from a behaving animal as stimulation patterns in studies of synaptic transmission (Dobrunz and Stevens, 1999). In the same spirit, we used a computational approach to investigate how a depressing or facilitating synapse would process complex spike trains similar to those occurring in the intact brain.

Although a fair number of modeling studies of short-term synaptic dynamics can be found in the literature, many of the existing biophysical models are concerned with a particular feature of synaptic response (Neher and Zucker, 1993; Tank *et al.*, 1995; Bertram *et al.*, 1996; Bennett *et al.*, 1997; Dobrunz and Stevens, 1997; Canepari and Cerubini, 1998; Wu and Betz, 1998), while models used in investigating the functional roles of short-term plasticity tend to be phenomenological (Tsodyks and Markram, 1997; Varela *et al.*, 1997, 1999). Furthermore, even the more detailed studies (Dittman and Regehr, 1998; Dittman *et al.*, 2000) do not take into account the stochastic nature of synaptic response, and only consider simple (periodic or Poisson) input patterns. In the present work, we investigated a model of synaptic dynamics that incorporates both the stochastic vesicle recycling process and activity-dependent facilitation. Unlike most existing models, our model takes into account the fundamental assumption, believed to hold for central synapses, that at most one vesicle can be released per action potential (Redman, 1990; Arancio *et al.*, 1994; Korn *et al.*, 1994; Stevens and Wang, 1995; Somogyi *et al.*, 1998; Walmsley *et al.*, 1998). This condition provides an important constraint on response properties of a cortical synapse. We explored the response of this model synapse to 'naturalistic' inputs similar to neuronal spike trains recorded *in vivo* from the cortex, and focused on two common kinds of complex neuronal firing patterns: spike trains containing fast bursts as well as isolated spikes, and spike trains of fractal temporal structure with long-term correlations.

Materials and Methods

Our synapse model is, in essence, a simple model of vesicle turnover (Fig. 1) (Wang, 1999; Matveev and Wang, 2000). It consists of a single vesicle pool of size N with an upper limit of N_0 , which can lose one vesicle in response to a presynaptic action potential. Depletion of the

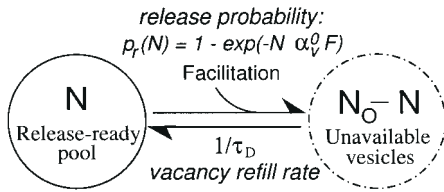


Figure 1. Model of vesicle turnover. Release probability is described by a Poisson process with lateral inhibition between individual vesicles during exocytosis, and is given by one minus the failure rate, which is equal to $\exp(-\alpha_v N)$, where $\alpha_v = \alpha_{v,0} F$ is the fusion rate for a single vesicle, and F is the facilitation factor. Vacancy in the vesicle pool is refilled with a time constant of τ_D , which determines the depression recovery dynamics.

vesicle pool leads to short-term depression, which recovers with a time constant τ_D equal to the inverse of the vacancy refill rate. Processes of vesicle release and recovery are treated stochastically (Vere-Jones, 1966; Melkonian and Kostopoulos, 1996; Quastel, 1997; Maass and Zador, 1999). Release of a single vesicle during an incoming pulse is governed by a Poisson process with some time-dependent rate $\lambda_v(t)$, which we assume is significant only for the duration of the pulse. The integral $\alpha_v = \int \lambda_v dt$ is the fusion rate for a single vesicle integrated over the duration of the presynaptic pulse. The single-vesicle release probability is then $p_v = 1 - \exp(-\alpha_v)$, and the single-vesicle failure probability is $1 - p_v = \exp(-\alpha_v)$ (Dobrunz and Stevens, 1997). Vesicle recovery is assumed to be governed by a Poisson process with rate $1/\tau_D$. Therefore, the probability for a vacancy in the vesicle pool to be refilled during a time interval Δt is given by $p_{\text{refill}} = 1 - \exp(-\Delta t/\tau_D)$.

We impose a constraint that no more than one vesicle can be released per single action potential, assuming that a vesicle release event transiently prevents other vesicles from being exocytosed, as suggested by Triller and Korn (Triller and Korn, 1982). Then, the release probability per stimulus is one minus the failure probability, given by the N th power of single-vesicle release failure probability, where N is the number of vesicles available for release (Dobrunz and Stevens, 1997, eq. 1.A):

$$p_r(N) = 1 - \exp(-\alpha_v N) \quad (1)$$

Therefore, the univesicular release constraint implies a nonlinear dependence of the release probability on the number of available vesicles. For a pool of synapses with a similar value of α_v , each with a different number of releasable vesicles N , the initial release probability p_r would increase with N according to equation (1) (see Fig. 5 of Dobrunz and Stevens, 1997).

We assume that the release site quickly recovers from the putative inhibition mechanism that prevents multivesicular release. As proposed by Dobrunz *et al.* (Dobrunz *et al.*, 1997), such a 'lateral inhibition' mechanism may be the basis for the observed brief refractory period following a postsynaptic response, during which the probability for another response to happen is small (Stevens and Wang, 1995; Hjelmstad *et al.*, 1997). Experimentally, one can distinguish between the relative and the absolute refractory times; for hippocampal synapses in culture, both values are close to 5 ms at room temperature (Stevens and Wang, 1995; Hjelmstad *et al.*, 1997), and decrease to ~ 3 – 4 ms at 31°C (Stevens and Wang, 1995). For our simulations, we set both time constants to 3 ms. After a spike the vesicle fusion rate α_v is set to zero for the duration of the absolute refractory time, after which α_v recovers exponentially with a time constant equal to the relative refractory time. Since these time constants are very short, at physiological firing rates the refractory period should affect only the synaptic response to fast bursts of action potentials.

Short-term Facilitation

We introduce facilitation into our model by allowing the vesicle fusion rate to increase with stimulation: $\alpha_v(t) = \alpha_{v,0} F(t)$, where $F(t)$ is the facilitation factor which is incremented with each incoming action potential according to a deterministic rule; this implies that we neglect the stochasticity resulting from probabilistic opening of presynaptic calcium channels (Bertram *et al.*, 1996; Bennett *et al.*, 1997). We assume that facilitation arises as a result of stimulation-induced increase in the

probability of release, due to a calcium-binding mechanism proposed by Bertram and colleagues (Bertram *et al.*, 1996). According to this model, each release site is controlled by four independent calcium gates, consistent with the fourth-order cooperativity between presynaptic Ca^{2+} concentration and synaptic response (Dodge and Rahamimoff, 1967). In order for exocytosis to take place, each of the gates has to open by binding a Ca^{2+} ion. All gates are assumed to have different kinetics, which is suggested by evidence of stepwise increase in facilitation with increasing stimulus frequency at the squid giant synapse, accompanied by a decrease in the Ca^{2+} co-operativity of release (Stanley, 1986). Multiple facilitation time scales have also been observed at cortical synapses (Dobrunz *et al.*, 1997; Thomson, 1997). One of the gates is assumed to have unbinding kinetics in the sub-millisecond range (Bertram *et al.*, 1996), so it should not contribute to facilitation (at physiological firing rates). Facilitation thus involves only three gates. The probability of a gate of type j remaining open then evolves according to a simple equation

$$\frac{dO_j}{dt} = k_j^+ [\text{Ca}^{2+}] (1 - O_j) - k_j^- O_j, \quad j = 1, 2, 3 \quad (2)$$

where Ca^{2+} influx is assumed to be brief, $[\text{Ca}^{2+}] = A_{\text{Ca}} \sum_i \delta(t - t_i)$, with t_i the arrival time of the i th stimulus. The parameters k_j^+ and $k_j^- = 1/\tau_{Fj}$ are respectively binding and unbinding kinetic coefficients for gate j . Time constants τ_{Fj} specify the decay times of the corresponding facilitation components. For simplicity, we assume that the vesicle release probability for a given action potential is determined by the states of release gates at the *end* of the spike. Let us denote by $O_j(t_n^+)$ the j th gating variable at the end of the n th spike, then the facilitation factor is $F(t_n) = F_1(t_n)F_2(t_n)F_3(t_n)$, where $F_j(t_n) = O_j(t_n^+)/O_j(t_1^+)$, $j = 1, 2, 3$. The vesicle fusion rate $\alpha_v(t_n) = \alpha_{v,0} F(t_n)$, where $\alpha_{v,0} \equiv \alpha_v(t_1)$ is the initial vesicle fusion rate.

The facilitation factors are updated as follows, for an arbitrary input train: (i) at the time of spike arrival, facilitation factors are incremented according to $F_j \rightarrow 1 + C_j F_j$, where $C_j = \exp(-A_{\text{Ca}} k_j^+)$ ($0 \leq C_j \leq 1$); (ii) between spikes each F_j recovers to 1 with time constant τ_{Fj} ($j = 1, 2, 3$). This update rule is based on the analytic solution of equation (2), linking values of gating variables for two successive spikes, t_n and t_{n+1} (Bertram *et al.*, 1996):

$$O_j(t_{n+1}^+) = O_j(t_1^+) + C_j e^{-(t_{n+1}-t_n)/\tau_{Fj}} O_j(t_n^+), \quad j = 1, 2, 3 \quad (3)$$

where $O_j(t_1^+) = 1 - C_j$ is the value after the first spike. Dividing by $O_j(t_1^+)$, we obtain the update rule for the facilitation factors:

$$F_j(t_{n+1}) = 1 + C_j e^{-(t_{n+1}-t_n)/\tau_{Fj}} F_j(t_n), \quad j = 1, 2, 3 \quad (4)$$

Note that the parameters C_j ($j = 1, 2, 3$) determine the facilitation strengths. From equation (4) follows that the paired-pulse facilitation (PPF) for very short interpulse intervals is given by $(1 + C_1)(1 + C_2)(1 + C_3)$; thus, the maximal paired-pulse facilitation that can be achieved within this model is $\text{PPF}_{\text{max}} = 2^p$, where $p = 3$ is the number of facilitation gates.

From equation (4) one finds that with constant-frequency stimulation of rate r , facilitation exponentially approaches a stationary level equal to

$$F_{\text{ss}} = \prod_{i=1,2,3} \frac{1}{1 - C_i \exp(-1/r\tau_{Fj})} \quad (5)$$

The associated steady-state vesicle fusion rate is $\alpha_{v,\text{ss}} = \alpha_{v,0} F_{\text{ss}}$.

Parameters

An important parameter of the synapse model is the number of vesicles in the release-ready pool, N_0 . The size of the release-ready pool varies across different types of central synapses (Zucker, 1996; Neher, 1998); we chose a range of values corresponding to hippocampal excitatory synapses, where recordings from individual boutons have been achieved (Bekkers and Stevens, 1990; Liu and Tsien, 1995; Forti *et al.*, 1997). For the rat hippocampal synapses in slice and culture, Stevens and collaborators assessed the size of the releasable pool by measuring the number of postsynaptic responses elicited by a short, high-frequency electric

stimulation (Stevens and Tsujimoto, 1995; Dobrunz and Stevens, 1997), or by a brief application of a hypertonic solution (Rosenmund and Stevens, 1996), as well as by optical monitoring of the amount of fluorescent dye uptaken and released during stimulation (Murthy *et al.*, 1997; Murthy and Stevens, 1998) [see also (Ryan *et al.*, 1997)]. The available pool size estimated in individual experiments varied between 2 and 25. Ultrastructural analysis of hippocampal synapses suggests that these numbers are consistent with the number of vesicles docked at single synaptic active zones (Forti *et al.*, 1997; Schikorski and Stevens, 1997). In our simulations we choose $N_0 = 3-10$. For the vesicle refill time constant we choose a value of $\tau_D = 1-2$ s, which agrees with the experimentally determined time of recovery of synaptic response from depression (Markram and Tsodyks, 1996; Dobrunz and Stevens, 1997; Varela *et al.*, 1997). Decay time constants for the three facilitation components are $\tau_{F1} = 35$ ms, $\tau_{F2} = 190$ ms and $\tau_{F3} = 2$ s. Quantitatively, the values of τ_{F1} and τ_{F2} were deduced from the interpulse-interval dependence of facilitation measured at hippocampal synapses by Dobrunz and co-workers (Dobrunz *et al.*, 1997) (see their Fig. 1). The value of the longer facilitation time constant τ_{F3} agrees with the facilitation recovery time at cortical pyramid-interneuron connections studied by Thomson (Thomson, 1997).

In this form, the model is specified by nine parameters: the maximal size of the vesicle pool N_0 , the depression recovery time constant τ_D , the initial fusion rate $\alpha_{v,0}$ [or, equivalently, the initial release probability $p_0 = 1 - \exp(-\alpha_{v,0}N_0)$], and the facilitation parameters C_j and τ_{Fj} , $j = 1, 2, 3$.

The magnitude of the initial release probability has been shown to determine the tendency of a given synapse to exhibit facilitation or depression of response (Debanne *et al.*, 1996; Dobrunz and Stevens, 1997; Tsodyks and Markram, 1997) [reviewed elsewhere (Korn and Faber, 1987; Zucker, 1989)]. Thus, we vary the values of p_0 (α_v), N_0 and C_j to achieve regimes of strong facilitation (low p_0 , high C_j) and strong depression (high p_0 , low N_0). In the regime of strong depression, facilitation cannot play a significant role since vesicle fusion rate α_v is already high; in this case we set $C_j = 0$ for the sake of simplicity.

Bursty Spike Train

To study the impact of short-term plasticity on synaptic response to bursts of spikes versus single spikes, we stimulate the model synapse with a spike train of high burst content. We generate such bursty spike train numerically, using a two-state pseudo-Markov process described by Ekholm and Hyvärinen (Ekholm and Hyvärinen, 1970) (Fig. 6A). In this process, firing alternates between two distinct modes or states: one of the states corresponds to a burst of spikes (high-frequency firing state), and the other corresponds to more sparsely spaced spikes between bursts (low-frequency firing state). This method produces spike sequences that are compatible with firing patterns observed in rabbit diencephalon and cat superior colliculus cells *in vivo* (Ekholm and Hyvärinen, 1970; Mandl 1993).

As in Ekholm and Hyvärinen (1970), the duration of a burst is determined by the number of interspike intervals (ISIs) within a burst, which obeys a binomial distribution $P_B(n)$. The interburst interval is determined by the number of ISIs between two consecutive bursts, which is drawn from a geometric distribution $P_S(n)$. The binomial distribution is given by

$$P_B(n+1) = \frac{m!}{n!(m-n)!} p_B^n (1-p_B)^{m-n}$$

$n = 0, \dots, m$, with parameter values $p_B = 0.5$ and $m = 8$. The geometric distribution is defined by $P_S(n+1) = (1-p_S)p_S^n$ ($n = 0, \dots, \infty$) with $p_S = 0.85$. Both distributions are shifted by one so that there is at least one ISI separating two bursts, and at least one ISI within a burst (i.e. at least two spikes per burst).

Interspike intervals within a burst (ISI_B) and between isolated spikes (ISI_S) are drawn from gamma probability densities of index 2 with different time constants:

$$\rho_{S,B}(t) = t^2 / (2\tau_{S,B}^3) \exp(-t/\tau_{S,B}) \quad (6)$$

where $\tau_B = 1.2$ ms corresponds to ISIs within bursts, and $\tau_S = 35$ ms corresponds to ISIs between bursts (average value of ISI_{S,B} is equal to $\tau_{S,B}$

multiplied by a factor of 3). This choice of probability densities leads to a bimodal ISI distribution similar to one seen in *in vivo* spike trains (Fig. 4B). We impose a lower bound on the minimal ISI by adding a dead time of 1 ms to all intervals. The average spike rate for these parameter choices is equal to 16.25 Hz.

To summarize, the spike train is generated by repeating the following sequence of steps: (i) the number of ISIs in a burst, m_B , is chosen according to probability distribution P_B ; (ii) burst is formed by generating m_B ISIs according to probability density ρ_B ; (iii) the number of long ISIs corresponding to single spikes between bursts, m_S , is drawn from probability distribution P_S ; (iv) m_S ISIs are chosen based on distribution ρ_S .

Fractal Spike Trains

To study the response of the synapse model to inputs with long-term temporal autocorrelations, we stimulate the model with numerically generated fractal spike trains. We generate such spike trains using the fractal shot-noise driven doubly stochastic Poisson process described by Lowen and Teich (Lowen and Teich, 1991). According to this process, probability of a spike occurring at time t is determined by a stochastically varying firing rate $r(t)$; namely, the probability of a spike occurrence within time interval $[t, t + \Delta t]$ is equal to $r(t)\Delta t$. The rate function $r(t)$ is constructed using another (primary) Poisson process of some constant rate r_0 . The event times $\{t_i\}$ of the primary Poisson process are passed through a linear filter $h(t)$, yielding rate function $r(t)$ of the fractal process:

$$r(t) = \sum_i h(K_i, t - t_i), \quad h(K, \tau) = \begin{cases} K\tau^{-\beta} & \text{if } T_A < \tau < T_B \\ 0 & \text{otherwise} \end{cases} \quad (7)$$

where amplitudes K_i are in general stochastic quantities. It is the power-law form of the filter function $h(t)$ that leads to long-term temporal correlations and the fractal nature of the process. Statistical quantities such as the autocorrelation function and the Fano factor (see definitions below) exhibit power-law temporal behavior for time-scales between T_A and T_B . Cut-offs T_A and T_B ensure that the spike rate $r(t)$ remains finite for any value of β .

We have chosen the following parameter values: $\beta = 0.9$, $T_A = 2$ ms, $T_B = 100$ s, $r_0 = 0.2$ Hz. Filter amplitude K_i is taken to be uniformly distributed between $K_A = 6$ and $K_B = 8$. To prevent events from occurring too close to each other, an absolute refractory time of 1.5 ms and a relative refractory time of 2 ms are imposed. Average event rate for these parameter choices is 14.7 Hz. The statistical properties of the resulting fractal spike train are shown in Figure 8.

Statistical Analysis: Temporal Autocorrelation

For a discrete (point) process such as a spike train, or a train of release events, autocorrelation function $G(\tau)$ characterizes the likelihood of observing two events separated by a time interval equal to τ . It is defined by

$$G(\tau) \equiv \lim_{\Delta t \rightarrow 0} \frac{P(\text{event in } [t + \tau, t + \tau + \Delta t] | \text{event in } [t, t + \Delta t])}{\Delta t} - \mu \quad (8)$$

where μ is the average event rate. In this normalization the autocorrelation function is therefore equal to the difference between the conditional probability rate of observing an event at (or close to) time $t + \tau$, given an event at (or close to) time t , and the average (unconditional) event rate μ . Here we assume that the process is stationary, so neither $G(\tau)$ nor μ depend on t . Autocorrelation function approaches zero as $\tau \rightarrow \infty$, since the correlation between the occurrences of two events should decrease as the time between the events grows.

Sometimes it may be convenient to normalize the autocorrelation by the average event rate; the resultant quantity is referred to as the coincidence rate: $g(\tau) = G(\tau)/\mu + 1$. The advantage of such a correlation measure is that it does not depend on the overall level of activity, i.e. it will not change if the event rate is modified by a constant factor.

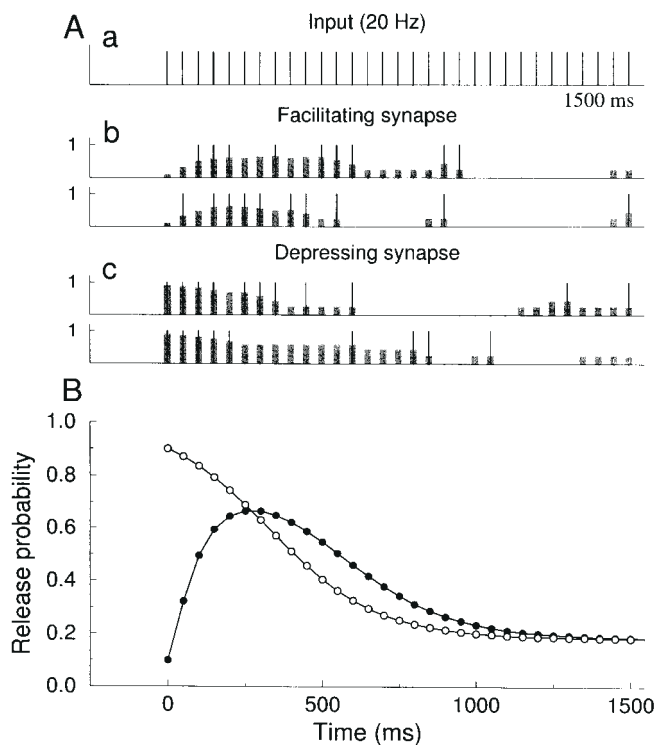


Figure 2. Response of the model to constant-frequency stimulation. (A) An example with a stimulus rate of 20 Hz; (a) stimulus train, (b) response in the facilitation regime, (c) response in the depression regime. In (b) and (c), two sample trials are shown. Black vertical bars represent release events; the height of the thick gray bars denotes the release probability at the time of arrival of a spike. Initial release probabilities are $p_0 = 0.1$ and $p_0 = 0.9$ for the facilitation and depression regimes respectively. For both cases, $N_0 = 8$ and $\tau_D = 2$ s. Facilitation parameters in (b) are $\tau_{F1,2,3} = 35$ ms, 190 ms, 2 sec; $C_{1,2,3} = 0.9, 0.95, 0.8$. (B) Trial-averaged release probability as a function of time in the facilitation (full circles) and depression (open circles) regimes. Same parameter values as in (A).

Statistical Analysis: the Fano Factor

The Fano factor characterizes the fluctuations of a point process, and is defined by the ratio of the variance and the mean of the number of events in a given time duration T (Fano, 1947):

$$F(T) = \frac{\text{var}[n(T)]}{\langle n(T) \rangle} \quad (9)$$

The Fano factor is equal to 1 for a Poisson process for any time interval T : in this case $\text{var}[n(T)] = \langle n(T) \rangle = \mu_T$, where μ is the average event rate. $F(T)$ is <1 for a process more regular than Poisson, and is >1 for a process with fluctuations larger than those in a Poisson process.

Results

Synaptic Response to Constant-frequency Stimulation

In response to a stimulus train, the model synapse may display either facilitation or depression of response, depending on values of model parameters. We choose two sets of parameter values, corresponding to regimes of strong facilitation and strong depression (Fig. 2). In each of these two regimes, the release probability and release event sequence are shown in Figure 2A for two sample trials of constant-frequency stimulation. Since only one release is allowed per action potential, synaptic output is a binary event sequence (release/failure). Toward the end of the traces there are periods of zero release probability, which are the times where the vesicle pool is completely depleted. The

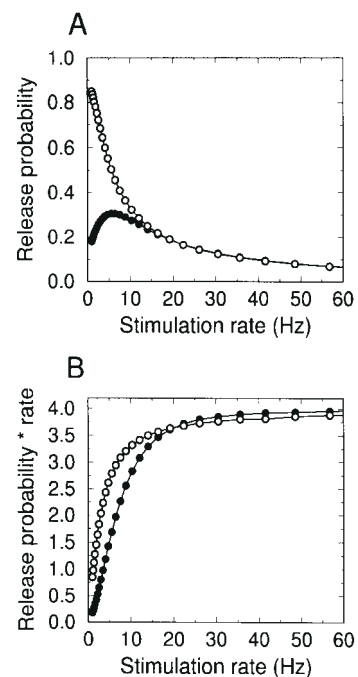


Figure 3. Dependence of steady-state synaptic response on the stimulation frequency. Curves with filled and open circles correspond to facilitation and depression regimes respectively. (A) Steady-state release probability. In the facilitation regime, release probability is non-monotonic, reaching a maximum at ~ 6 Hz. Parameter values are the same as in Figure 2. (B) Steady-state synaptic response rate, given by the product of the average release probability and stimulation rate. In both regimes, response amplitude reaches a plateau at high firing rates. The value of the plateau is insensitive to initial release probability and facilitation, but depends on N_0 and τ_D : $\langle p_r \rangle r \approx N_0 / \tau_D$.

trial-averaged release probability $\langle p_r \rangle$, which represents the average synaptic response per stimulus, is shown in Figure 2B. These time courses of short-term plasticity are similar to those observed experimentally in cortical synapses [cf. Fig. 2 in (Dobrunz and Stevens, 1997)].

In contrast to the depression regime where $\langle p_r \rangle$ decreases monotonically, in the case of facilitation $\langle p_r \rangle$ initially grows, until vesicle depletion takes over; for both regimes, release probability eventually approaches a stationary state, $\langle p_r \rangle_{ss}$. The characteristic time of response decay in the depression regime depends both on the recovery time constant τ_D and the rate of stimulation r , and is typically much shorter than τ_D . It is smaller with larger α_V or higher stimulation rate r (Wang, 1999; Matveev and Wang, 2000).

In Figure 3A, the steady-state release probability $\langle p_r(r) \rangle_{ss}$ is plotted as a function of the stimulation rate. In the facilitation regime, this dependence is non-monotonic, displaying a maximum near 6 Hz (Markram *et al.* 1998). However, in both cases the synaptic response rate, given by the product of $\langle p_r(r) \rangle_{ss}$ and the stimulation rate r , increases monotonically and approaches a plateau at high stimulation frequencies (Fig. 3B). The saturation of the response rate implies that the steady-state release probability decays as $1/r$ at high rates, due to vesicle depletion (Liley and North, 1952). Therefore, the response rate becomes insensitive to the frequency of sustained presynaptic stimulation at high input rates (Abbott *et al.*, 1997; Tsodyks and Markram, 1997).

Response to Bursty Spike Trains

Our synapse model can display various degrees of short-term

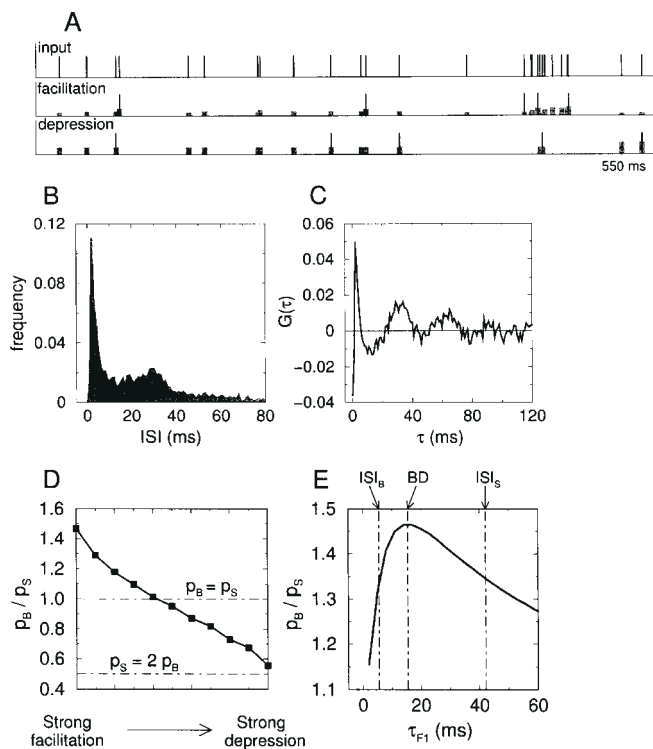


Figure 4. Response of the model synapse to a spike train recorded from the visual cortex of the awake monkey, in response to a grating stimulus (spike train provided by Charles Gray and Rony Azouz). (A) Trial responses to a segment of the spike train, in the facilitation and depression regimes. Thin lines: input spikes and synaptic release events; gray bars: release probability at the time of spike arrival. Parameters for the depression regime: $N_0 = 7$, $p_0 = 0.95$, $\tau_D = 1$ s; for the facilitation regime: $N_0 = 12$, $p_0 = 0.11$, $\tau_D = 1$ s, $C_{1,2} = 0.9, 0.95$; $\tau_{F1, F2} = 15, 190$ ms. Average stimulation rate is 38 Hz. Average release probabilities are $\langle p_r \rangle = 0.172$ in the facilitation and $\langle p_r \rangle = 0.170$ in the depression regimes. (B) Interspike interval histogram (ISIH) for the experimental spike train exhibits bimodal character. (C) Autocorrelation function reveals oscillations around 32 Hz. (D) The ratio of release probabilities for a spike in a burst (p_B) and an isolated spike (p_S), as a function of short-term synaptic plasticity. Parameters are varied linearly from strong facilitation ($N_0 = 12$, $p_0 = 0.05$, $C_1 = 0.9$, $C_2 = 0.7$) to strong depression regime ($N_0 = 3$, $p_0 = 0.95$, $C_1 = C_2 = 0$). Time constants are not varied ($\tau_D = 1$ s, $\tau_{F1} = 15$ ms, $\tau_{F2} = 190$ ms). (E) Dependence of the p_B/p_S ratio, in the regime of strong facilitation, on the fast facilitation time constant τ_{F1} , with other parameters kept fixed. This ratio shows a peak at $\tau_{F1} \approx$ average burst duration (BD = 15.4 ms). The average ISI within a burst $ISI_B = 5.5$ ms, and the average interval between single spikes and between isolated spikes and bursts $ISI_S = 42.2$ ms.

facilitation and depression, depending on the choice of parameters. As we have seen above, in response to a constant-frequency input train, the behavior of the synapse in regimes of strong facilitation and depression differs dramatically only during the initial few stimuli, but not in the steady state (Figs 2B, 3B). The situation, however, is different for more complex input patterns. When the stimulation train possesses a rich temporal structure, the input rate is constantly changing in time, which unceasingly modifies the internal state of the synapse due to activity-dependent, short-term plasticity, and the output is expected to be different at a strongly facilitating synapse compared to a strongly depressing synapse. Here we test this idea using real spike trains recorded *in vivo* from cortical cells, as well as spike sequences generated numerically.

Neuronal firing patterns recorded from different cortical areas of both anesthetized and behaving animals reveal a rich temporal structure: periods of rapid firing alternate with periods of relative inactivity, and bursts of closely spaced spikes are often

observed along with spikes separated by longer time intervals (Bair *et al.* 1994; Gray and McCormick, 1996). It is conceivable that short-term plasticity could allow the synapse to select specific temporal features from the input spike train for transmission to the postsynaptic neuron. For instance, Lisman suggested that facilitation enables synapses to respond reliably to bursts of spikes, which might contain most of the information carried by the spike train, while filtering out stand-alone tonic spikes that could represent unwanted noise (Lisman, 1997). An alternative possibility is that bursts and single spikes could code for different features of the same stimulus (Cattaneo *et al.*, 1981; DeBusk *et al.*, 1997).

Here we study quantitatively the ability of the model synapse to detect bursts by analyzing its response to burst-rich stimulus trains. As a specific example, we drive the model with a spike train recorded in the visual cortex of the awake monkey, in response to a grating stimulus (Fig. 4A). This cell displays ‘chattering’ behavior (Gray and McCormick, 1996; Wang, 1999), firing bursts and single spikes rhythmically; the ISI histogram is bimodal (Fig. 4B) and the autocorrelation function for the given cell shows a pronounced oscillatory component in the 30–35 Hz frequency range (Fig. 4C). As seen in Figure 4A, in the facilitation regime the release probability is substantially enhanced within a burst of spikes. By contrast, in the depression regime the release probability is typically reduced within a burst due to vesicle depletion. In Figure 4A the time-averaged release probability $\langle p_r \rangle$ is about the same in the depressing and facilitating cases.

To characterize the ability of the synapse to detect bursts, we calculate separately the release probability for a single spike (p_S) (i.e. fraction of single spikes that lead to a vesicle release) and that for a spike within a burst (p_B). The ratio between these two values, p_B/p_S , is calculated for different model parameters covering a continuous range from the strong facilitation regime to the strong depression regime. A burst spike is defined as a spike that is preceded or followed by another spike within a short time interval of 10–15 ms; this interval corresponds to the trough in the bimodal ISI distribution (such as one seen in Fig. 4B). In this definition burst spikes correspond to the short ISI mode in the ISI distribution.

Since we are mostly interested in spike trains with relatively high spike rates (>10 Hz), we reduce the number of facilitation processes to two, assuming that the slowest facilitation component is close to saturation at high firing frequencies, and does not significantly affect the character of synaptic response. As can be seen in Figure 4, we find that in the case of strong facilitation, the synapse can be 50% more likely to respond to an incoming spike if it belongs to a burst. Conversely, in the strong depression case, synapse is almost twice as likely to respond to a single spike than a spike within a burst, since vesicle depletion makes multiple release events during a single burst less probable. For a certain intermediate plasticity regime, facilitation balances depression, and the release probability is the same for any spike.

Naturally, this ability of the synapse to discriminate the bursts depends crucially on the facilitation time constants, especially the shortest one τ_{F1} . The effect is expected to be optimal if τ_{F1} is shorter than the average interval between single spikes and between a single spike and a burst (so that facilitation decays away between single spikes), but significantly longer than the ISIs within a burst (so that facilitation accumulates during a burst). This is demonstrated in Figure 4E, where the behavior of the release probability ratio p_B/p_S is shown as a function of τ_{F1} . One can see that the maximal burst discrimination is achieved when the facilitation decay time matches the average burst

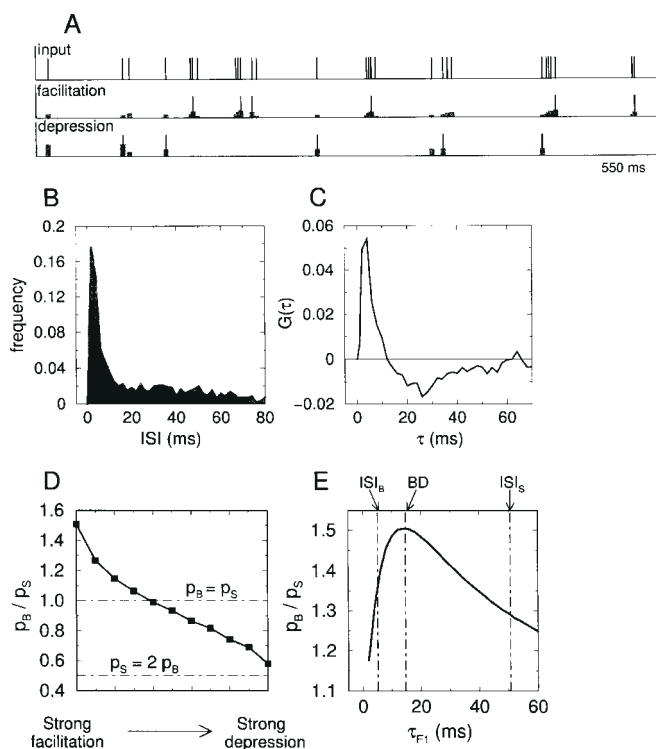


Figure 5. Response of the model synapse to a spike train recorded from a neuron in the monkey prefrontal cortex during the delay period in an oculomotor delayed-response memory task (spike train provided by Matt Chafee and Patricia Goldman-Rakic). (A) Trial responses to a segment of the spike train, in the facilitation and depression regimes. Synaptic parameters same as in Figure 4A. Average stimulation rate is 36 Hz. Average release probabilities are $\langle p_i \rangle = 0.182$ in the facilitation and $\langle p_i \rangle = 0.186$ in the depression regimes. (B) Interspike interval histogram and (C) autocorrelation function for the experimental spike train. (D) The ratio of release probabilities for a spike in a burst (p_B) and an isolated spike (p_S), as a function of short-term synaptic plasticity. Conventions and parameters same as in Figure 4D. (E) Dependence of the p_B/p_S ratio, in the regime of strong facilitation, on the fast facilitation time constant τ_{F1} , with other parameters kept fixed. This ratio shows a peak at $\tau_{F1} \approx$ average burst duration (BD = 14.7 ms). The average ISI within a burst $ISI_B = 5.1$ ms, and the average interval between single spikes and between isolated spikes and bursts $ISI_S = 50.7$ ms.

duration. For the same reason, the p_B/p_S ratio will be greater if the second facilitation time constant, τ_{F2} , is smaller and closer to the average burst duration.

A second example is a bursty spike train recorded from the monkey prefrontal cortex during the delayed period of an oculomotor delayed response task (Fig. 5A); it thus represents mnemonic neuronal activity correlated with working memory (Chafee and Goldman-Rakic, 1998). This cell shows a strong propensity to fire brief bursts of spikes, as evidenced by visual inspection of the spike train shown in Figure 5A and by the peak in the ISIH at very short intervals (Fig. 5B). This cell displays a strong positive autocorrelation at short temporal scale (Liu *et al.*, 1998), as demonstrated by the large peak in the autocorrelogram (Fig. 5C), but does not exhibit oscillatory behavior. Similarly to the case of the chattering cell from the visual cortex, we found that for a facilitating synapse the release probability is significantly higher for a spike belonging to a burst than for an isolated spike; the opposite is true for a depressing synapse (Fig. 5A). The p_B/p_S ratio is 1.5 in the strongly facilitating regime, and 0.55 in the strongly depressing regime (Fig. 5D). Again, the burst detectability is optimal if there is a match between the time constant of short-term facilitation and the mean burst duration (Fig. 5E).

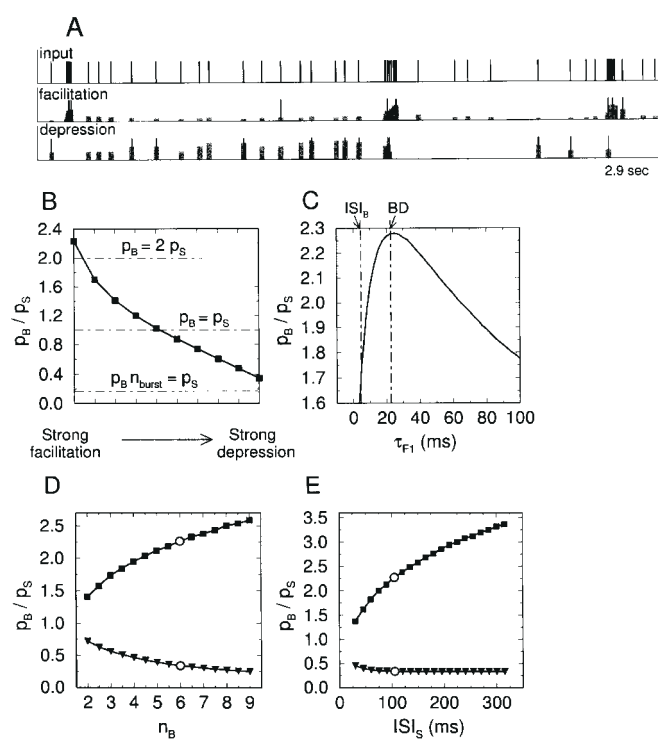


Figure 6. Response of the model synapse to a burst-rich spike train generated according to a two-state stochastic process (Ekholm and Hyvärinen, 1970). (A) Trial responses to a 2.9 s segment of the spike train. The average number of spikes in a burst is $n_{burst} = 6$; average number of single spikes between bursts is $n_{single} = 5.7$; average firing rate is 16 Hz. Conventions and parameters same as in Figure 4A. (B) Burst-discriminating ability as a function of synaptic parameters. Conventions same as in Figure 4D. Parameters are varied linearly left to right from strong facilitation values ($N_0 = 12$, $p_0 = 0.07$, $C_1 = 0.9$, $C_2 = 0.95$) to strong depression values ($N_0 = 3$, $p_0 = 0.92$, $C_1 = C_2 = 0$). Time constants are not varied ($\tau_0 = 2$ s, $\tau_{F1} = 35$ ms, $\tau_{F2} = 190$ ms). (C) Burst-discriminating ability of a strongly facilitating synapse as a function of the facilitation time constant τ_{F1} . Conventions same as in Figure 4E. Vertical lines mark the duration of the ISI within a burst ($ISI_B = 4.5$ ms) and the average burst duration (BD = 22.5 ms). The average interval between stand-alone spikes and between a single spike and a burst is $ISI_S = 105$ ms. (D) Burst-discriminating ability of a strongly facilitating (squares) and a strongly depressing (triangles) synapse as a function of the number of spikes per burst. Average firing rate varies from 10.9 to 19.5 Hz as n_B is increased from 2 to 9. Open circles correspond to $n_B = 6$ used in (A)–(C), (E). (E) Burst-discriminating ability of a strongly facilitating (squares) and a strongly depressing (triangles) synapse as a function of the average interval between isolated spikes, ISI_S . Average firing rate varies from 53.5 to 5.5 Hz over the range of ISI_S covered in this plot ($ISI_S = 30$ –315 ms). Open circles mark $ISI_S = 105$ ms used in (A)–(D).

Therefore, our conclusion about the optimal facilitation time constant for burst discrimination is rather general and is not limited to a particular type of burst-containing spike train. To further confirm this point, we also considered artificial random bursty spike trains generated numerically according to a pseudo-Markov stochastic process (see Materials and Methods, and Fig. 6A). In this case the burst-discriminating ability of the synapse in the facilitating regime is significantly higher (Fig. 6B,C), and the release probability for a spike within a burst is almost twice as high as that for an isolated spike. As in the case of spike trains recorded *in vivo*, the p_B/p_S ratio is maximized when the dominant facilitation time constant matches the average burst duration (Fig. 6C). The greater burst discrimination is realized because of the larger average number of spikes within a burst (6 compared to 2–3 for the chattering cell spike train), and longer average interval between bursts and stand-alone spikes. Thus, the average number of spikes in a burst and

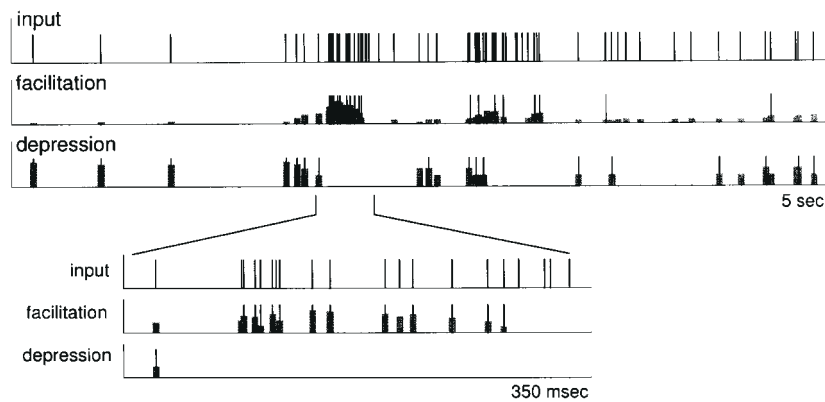


Figure 7. A sample spike train generated according to the fractal shot-noise driven doubly stochastic Poisson process (Lowen and Teich, 1991) and synaptic responses for the strong facilitation and depression regimes. Average input spike rate is $r = 14.7$ Hz. Synaptic parameters are $N_0 = 7$, $\tau_D = 2$ s, $p_0 = 0.95$ for the depression regime, and $N_0 = 12$, $\tau_D = 2$ s, $p_0 = 0.11$; $\tau_{F1,2} = 35, 190$ ms; $C_{1,2} = 0.9, 0.95$ for the facilitation regime. Average release probabilities are $\langle p_i \rangle = 0.211$ for the facilitation regime and $\langle p_i \rangle = 0.230$ for the depression regime. The inset shows a cluster in the input spike train with greater resolution. Note the dramatic increase of the release probability during a cluster in the facilitation regime.

the stimulation ‘duty cycle’ are parameters that critically determine the ability of the synapse to detect bursts in the given stimulation pattern. This is demonstrated in Figure 6, where the ratio of release probabilities for a burst spike and a single spike is shown to increase monotonically as a function of the number of spikes per burst (Fig. 6D), and the length of the interval between isolated spikes (Fig. 6E).

Variation of the depression recovery time parameter has a much weaker effect on the burst discrimination ability of the model synapse. Changing τ_D from 1 to 4 s leads to an increase in the p_B/p_S ratio of at most 30%, with significant increase taking place only under conditions of strong facilitation and large n_B (simulation results not shown). This is because in the absence of facilitation an increase in τ_D causes comparable decrease in both p_B (response to a burst spike) and p_S (response to a single spike), but strong facilitation partially compensates for stronger depression during a burst.

Response to Fractal Spike Trains

It has been traditionally assumed that a sequence of action potentials produced by a firing neuron can be accurately represented by a ‘memoryless’ stochastic Poisson process, in which individual ISIs are statistically independent of each other (Mueller, 1954; Kuffler *et al.*, 1957; Bishop *et al.*, 1964; Smith and Smith, 1965). However, it has been established that long sequences of action potentials recorded in a variety of neural systems exhibit considerable long-term autocorrelations and reveal fractal (self-similar) temporal structure, characterized by the power-law scaling of autocorrelation with time and $1/f$ behavior of the power spectrum. This effect has been observed in visual and auditory systems of vertebrates and invertebrates (Teich, 1989, 1992; Turcott *et al.*, 1995; Lowen and Teich, 1996; Teich *et al.*, 1997), in somatosensory cortex (Wise, 1981), and reticular formation neurons (Grüneis *et al.*, 1993). Thus, it appears that this property of neural firing is common and it is therefore of interest to study how the statistics of such self-similar signals are modified by short-term synaptic dynamics. For this purpose we have generated a fractal spike train according to the fractal shot-noise driven doubly stochastic Poisson model (see Materials and Methods), and used it as an input to the model synapse. As shown in Figure 7, in response to such a fractal spike train, the output of the synapse model is dramatically different in the facilitation and depression regimes.

For a fair comparison, the overall average release probability is adjusted to be the same in these two cases, so that the distinct statistics of the output patterns must be accounted for by the difference in the synaptic temporal dynamics rather than in the average transmission efficiency. For a facilitating synapse, the release probability is very small for an isolated spike, but is greatly increased during a cluster of spikes, whereas for a depressing synapse the release probability is significant for an isolated spike, but usually decreases to zero during a cluster of spikes due to vesicle depletion. Therefore, facilitation is expected to enhance temporal autocorrelation of the release event sequence at relatively short term scales (e.g. within a cluster), whereas depression should reduce the autocorrelation.

Statistical properties of the input stimulus train and output release trains are compared in Figure 8. In Figure 8A the interstimulus interval histogram (ISIH) is superimposed with the output interrelease interval histogram (IRIH). Note the much larger probability of short IRIs in the facilitation regime than in the depression regime. Also, the probability is larger for IRIs than for ISIs at long time intervals, because synaptic transmission is not reliable (overall average release probability is 0.15 and 0.17 for the facilitating and depressing regimes respectively) so that the mean IRI is longer than the mean ISI. Figure 8B shows the Fano factor, which characterizes the temporal fluctuations of event counts at different time-scales. For the fractal input train, the Fano factor grows with time, which reflects the presence of spike-count variations at all time-scales. The Fano factor of the release event sequence remains close to unity at all time-scales in the depression regime, which is expected for a Poisson process with spike count variance equal to its mean. Even in the facilitation regime, the Fano factor is greatly reduced compared to its value for the input spike train, especially at time-scales of 1 s and beyond. Therefore, synaptic depression leads to the reduction of high variability present in the input. We note that these results also apply to the statistical properties of combined response of several synaptic connections, since release events at different synapses are statistically independent. For instance, the temporal autocorrelation of the postsynaptic response will be equal to the sum of response autocorrelations of individual synapses.

The decorrelation effect of short-term synaptic plasticity is quantified by comparing the temporal correlation and power spectrum of the synaptic output to those of the fractal input (Fig.

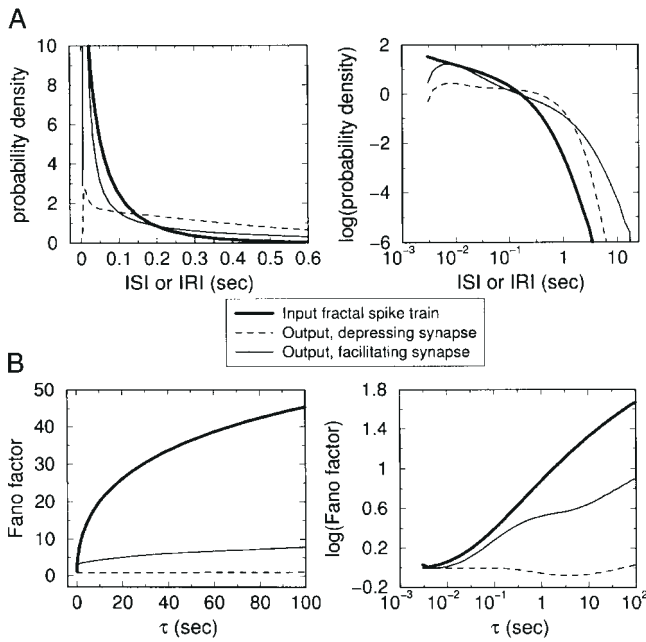


Figure 8. Interval distribution and variability of a fractal signal before and after transmission through a model synapse. Both linear and log–log plots are given for each curve. Thick solid lines: presynaptic spike train; thin solid and dashed lines: output release event sequences for facilitation and depression regimes respectively. (A) Comparison of ISI distribution with the interrelease event interval distributions. (B) Fano factors for the fractal input and the synaptic outputs. For the fractal input, away from the upper and lower cut-offs the Fano factor behaves as $F(T) \sim 1 + cT^{2(1-\beta)}$, where $\beta = 0.9$, and c is a constant. In the depression regime the Fano factor of the output release train is close to 1, as expected for a totally uncorrelated Poisson train. (Synaptic parameters are $N_0 = 5$, $\tau_D = 2$ s, $\rho_0 = 0.9$ for the depression regime, and $N_0 = 8$, $\tau_D = 2$ s, $\rho_0 = 0.02$; $\tau_{f1,2,3} = 35$ ms, 190 ms, 2 s; $C_{1,2,3} = 0.9, 0.95, 0.8$ for the facilitation regime.)

9). For the fractal input train, both temporal correlation and power spectrum display power laws in time (manifested by the linear regions in log–log plots, Fig. 9). As expected, short-term synaptic facilitation leads to an increase in autocorrelation magnitude at short time-scales, while depression dramatically reduces correlations (Fig. 9A). The dip in the millisecond time range results from refractoriness of vesicle release. Even in the facilitation regime, the long-term temporal correlations that are a hallmark of fractal signals are reduced at time-scales longer than several hundred milliseconds. The power spectrum of the output train is virtually flat for both facilitating and depressing synapses (Fig. 9B), in this sense we can say that short-term synaptic depression can effectively ‘whiten’ the input, and reduce strong redundancies present in the inputs in the form of temporal correlations. Goldman and colleagues have previously shown a decorrelation effect by synaptic depression in the case where the input train has a correlation time of a few hundreds of milliseconds (Goldman *et al.*, 1999). Here, it is demonstrated that this synapse-specific mechanism can even decorrelate fractal-like inputs with correlations at all time-scales.

Discussion

The present model study was partly motivated by the recent experimental finding that short-term synaptic plasticity is differentially expressed in cortex: some synapses show strong depression while others express pronounced facilitation (Thomson, 1997; Thomson and Deuchars, 1997; Markram *et al.*, 1998; Reyes *et al.*, 1998; Varela *et al.*, 1999). To shed light on the

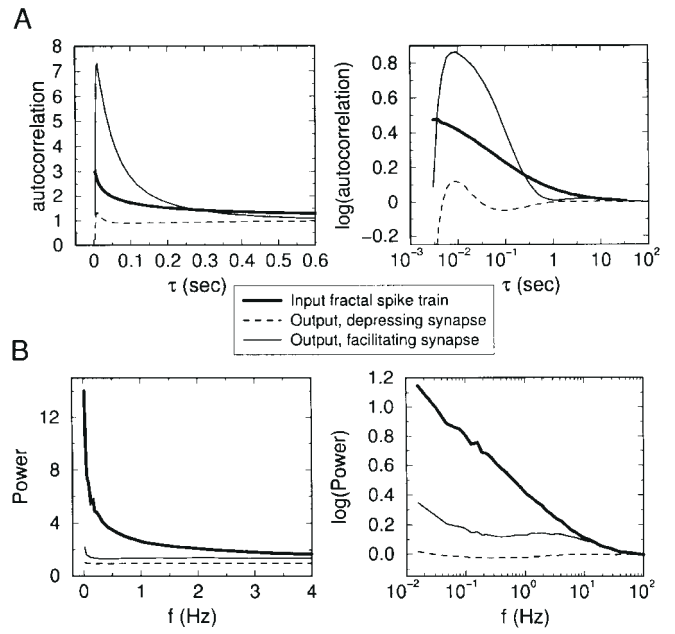


Figure 9. Temporal correlation and power spectrum of a fractal signal before and after transmission through a model synapse. Conventions and parameters same as in Figure 8. (A) Autocorrelation for the fractal signal and the synaptic output. Sharp decline at small time scales is due to the refractory time. (B) Power spectral density for the fractal input and the synaptic outputs. For the fractal input, away from the upper and lower cut-offs the autocorrelation is approximated by $g(\tau) \approx 1 + \bar{c}\tau^{-2\beta}$, and the power spectrum behaves as $S(f) \approx 1 + cf^{-2(1-\beta)}$, where $\beta = 0.9$, and c, \bar{c} are constants. In the depression regime, the input signal is decorrelated by the synaptic dynamics, and the power spectrum of the output release train becomes flat (‘whitened’).

computational implications of this differential short-term plasticity, we used a stochastic model of short-term synaptic dynamics and investigated how a facilitating or depressing synapse would respond to complex stimuli similar to those occurring in the intact brain. Our synapse model includes a vesicle turnover process and a facilitation mechanism, with the constraint that at most one vesicle can be released per stimulus (Triller and Korn, 1982; Redman, 1990; Korn and Faber, 1991; Korn *et al.*, 1994; Stevens and Wang, 1995).

It has been proposed that bursts of spikes and isolated spikes in a neuronal spike train could differ in the extent and kind of information that they provide about the external stimulus. For example, it has been reported that orientation of a visual stimulus is encoded in the burst component of the firing discharges in visual cortical neurons, while the isolated spike component is correlated with the contrast of the stimulus (Cattaneo *et al.*, 1981; Livingstone, 1996; DeBusk *et al.*, 1997). For motion-sensitive visual cells of the cat superior colliculus, evidence suggests that stimulus velocity is encoded in relative durations of bursting versus ‘resting’ (low-frequency) episodes (Mandl, 1993). If bursts and isolated spikes encode different types of information, then it would be important for a synapse to be able to respond differently to isolated spikes and spikes within a burst, thereby selecting the type of information that is transmitted to the postsynaptic neuron. To study this possibility, we have analyzed the ability of a facilitating synapse to respond preferentially to bursts of action potentials (Lisman, 1996; Thomson, 1997; Wang, 1999). This was done by driving the synapse model with burst-rich spike trains recorded from visual (Fig. 4) and prefrontal cortices (Fig. 5) of awake and behaving

monkeys, and with artificially generated spike trains (Fig. 6). We quantified the burst discrimination capability of the synapse by the ratio between the release probability for a spike within a burst (p_B) and that for an isolated spike (p_S). It was found that p_B/p_S can be as much as five times higher for a highly facilitating synapse than for a strongly depressing synapse (Fig. 6C). We identified two quantitative conditions for optimal burst discrimination by a plastic synapse. First, the effect is maximized when the facilitation time constant matches the average burst duration (Figs 4E, 5E, 6C). Second, burst discrimination can only be achieved for spike trains with a high number of spikes per burst (so that there is significant facilitation during a burst; see Fig. 6D), and long time intervals between two consecutive bursts or between a burst and a single spike (so that facilitation decays away between two spikes not belonging to the same burst; see Fig. 6E). The existence of several facilitation components with disparate decay times points to the possibility that a synapse may be tuned to detect temporal clustering of spikes in the presynaptic stimulation train at several distinct time-scales. How an optimal match between the facilitation kinetics (a synaptic property) and the characteristics of the bursty spike train (a neuronal property) could be achieved in a neural system remains an open question.

Neuronal spike patterns recorded in a variety of neural systems were shown to possess self-similar temporal structure, characterized by long-lasting correlations (Teich, 1992; Lowen *et al.*, 1997). We analyzed the effects of short-term plasticity on transmission of such fractal inputs using numerically generated spike trains. We found that facilitation enhances correlations present in the presynaptic stimulation pattern, at short time-scales. On the other hand, depression drastically reduces correlations in the release sequence at all time-scales and destroys the power-law scaling of the output autocorrelation (Fig. 8). This result agrees with and extends the conclusions of the previous work (Goldman *et al.*, 1999), which reported decorrelation by a depressing synapse model of an input train with a characteristic correlation time constant of a few hundreds of milliseconds. Statistical analysis revealed that sensory inputs from the external world display correlations at all scales according to fractal-like scaling laws (Ruderman, 1994; van Hateren, 1997). It has been suggested that neural coding efficiency of sensory inputs could be enhanced by a reduction in input redundancy (i.e. strong correlations) (Barlow, 1961; Atick, 1992; Goldman *et al.*, 1999). The present work demonstrates that short-term synaptic depression is able to remove temporal correlations at all scales and 'whiten' fractal-like inputs. Correlations could be preserved or even enhanced at short time-scales if a synapse also displays activity-dependent facilitation. Therefore, decorrelation and redundancy reduction may not necessarily exclude the presence of correlations at shorter time scales (from a few to a few hundreds of milliseconds) which is often seen in cortical neurons (Abeles *et al.*, 1994; Gray, 1999; Singer, 1999).

Our theoretical predictions could be tested by using fractal-like stimulation train in studies of synaptic transmission in cortex. A more indirect approach would be to compare temporal autocorrelations of two monosynaptically connected neurons along a sensory pathway. Such a comparison was done for the cat retinal ganglion cells and neurons in the lateral geniculate nucleus, during spontaneous discharges (Teich *et al.*, 1997). It was found that fractal-like temporal statistics are similar in both cell populations, suggesting minimal decorrelation effect at the retino-geniculate synapses. On the other hand, the study by

Teich and colleagues also indicates that fractal-like long-term correlations could be generated intrinsically in the visual system, since the activities recorded were spontaneous in the absence of visual stimuli (Teich *et al.*, 1997). Long-term correlations could be introduced by internal cellular mechanisms acting either at the synaptic level or at the level of spike generation (Teich, 1992). Indeed, analysis of exocytic events at neuromuscular junctions and at the rat hippocampal synapses in culture provided evidence for fractal-like scaling in the rate of spontaneous release events (Lowen *et al.*, 1997). If the self-similar behavior is caused by intracellular mechanisms acting predominantly at the synaptic level, this could indicate that short-term plasticity itself displays fractal properties, and the decay of some facilitation and depression components could be power-law rather than exponential in time.

There is evidence that depression mechanisms beyond vesicle depletion contribute to the short-term depression observed at central synapses (Bellingham and Walmsley, 1999). For instance, depression may result from calcium-dependent inactivation of exocytosis machinery (Hsu *et al.*, 1996; Matveev and Wang, 2000). Such an effect would further decrease the p_B/p_S ratio in the response of the depressing synapse to bursty spike trains, and would strengthen the decorrelation effect of short-term depression described here. We have chosen not to incorporate this inactivation mechanism into our model since it would not affect the main conclusions of this work, and would require including parameters with values that are currently not constrained by experimental data.

Notes

We thank Larry Abbott, Sacha Nelson, Venkatesh Murthy and Charles Stevens for discussions and helpful comments on the manuscript. We are grateful to Charles Gray, Rony Azouz, Patricia Goldman-Rakic and Matt Chaffee for providing experimental recordings of cortical spike trains. This work was supported by the Alfred P. Sloan Foundation, and the National Institutes of Health Grant MH53717-01.

Address correspondence to Xiao-Jing Wang, Volen Center for Complex Systems, Brandeis University, Waltham, MA 02454, USA. Email: xjwang@volen.brandeis.edu.

References

- Abbott LF, Varela JA, Sen K, Nelson SB (1997) Synaptic depression and cortical gain control. *Science* 275:220-224.
- Abeles M, Prut Y, Bergman H and Vaadia E (1994) Synchronization in neuronal transmission and its importance for information processing. *Progr Brain Res* 102:395-404.
- Ali AB, Thomson AM (1998) Facilitating pyramid to horizontal oriens-alveus interneurone inputs: dual intracellular recordings in slices of rat hippocampus. *J Physiol* 507:185-199.
- Ali AB, Deuchars J, Pawelzik H, Thomson AM (1998) CA1 pyramidal to basket and bistratified cell EPSPs: dual intracellular recordings in rat hippocampal slices. *J Physiol* 507:201-217.
- Arancio O, Korn H, Gulyas A, Freund T, Miles R (1994) Excitatory synaptic connections onto rat hippocampal inhibitory cells may involve a single transmitter release site. *J Physiol* 481:395-405.
- Atick JJ (1992) Could information theory provide an ecological theory of sensory processing? *Network* 3:213-251.
- Bair W, Koch C, Newsome W, Britten K (1994) Power spectrum analysis of bursting cells in area MT in the behaving monkey. *J Neurosci* 14:2870-2892.
- Barlow HB (1961) Possible principles underlying the transformations of sensory messages. In: *Sensory communication* (Rosenblith WA, ed.), pp. 217-234. Cambridge, MA: MIT Press.
- Bekkers JM, Stevens CF (1990) Presynaptic mechanism for long-term potentiation in the hippocampus. *Nature* 346:724-729.
- Bellingham MC, Walmsley B (1999) A novel presynaptic inhibitory mechanism underlies paired pulse depression at a fast central synapse. *Neuron* 23:159-170.
- Bennett MR, Gibson WG, Robinson J (1997) Probabilistic secretion of

- quanta and the synaptosecretosome hypothesis: evoked release at active zones of varicosities, boutons, and endplates. *Biophys J* 73:1815-1829.
- Bertram R, Sherman A, Stanley EF (1996) Single-domain/bound calcium hypothesis of transmitter release and facilitation. *J Neurophysiol* 75:1919-1931.
- Bishop PO, Levick WR, Williams WO (1964) Statistical analysis of the dark discharges of lateral geniculate neurones. *J Physiol* 170:598-612.
- Buhl EH, Tamas G, Szilagy T, Stricker C, Paulsen O, Somogyi P (1997) Effect, number and location of synapses made by single pyramidal cells onto aspiny interneurons of cat visual cortex. *J Physiol* 500:689-713.
- Buonomano DV (2000) Decoding temporal information: a model based on short-term synaptic plasticity. *J Neurosci* 20:1129-1141.
- Buonomano DV, Merzenich MM (1995) Temporal information transformed into a spatial code by a neural network with realistic properties. *Science* 267:1028-1030.
- Canepari M, Cherubini E (1998) Dynamics of excitatory transmitter release: analysis of synaptic responses in CA3 hippocampal neurons after repetitive stimulation of afferent fibers. *J Neurophysiol* 79:1977-1988.
- Castro-Alamancos MA, Connors BW (1997) Distinct forms of short-term plasticity at excitatory synapses of hippocampus and neocortex. *Proc Natl Acad Sci USA* 94:4161-4166.
- Cattaneo A, Maffei L, Morrone C (1981) Two firing patterns in the discharge of complex cells encoding different attributes of the visual stimulus. *Exp Brain Res* 43:115-118.
- Chafee MV and Goldman-Rakic PS (1998) Neuronal activity in macaque prefrontal area 8a and posterior parietal area 7ip related to memory guided saccades. *J Neurophysiol* 79:2919-2940.
- Debanne D, Guéroux NC, Gähwiler BH, Thompson SM (1996) Paired-pulse facilitation and depression at unitary synapses in rat hippocampus: quantal fluctuation affects subsequent release. *J Physiol* 491(part 1):163-176.
- DeBusk BC, DeBruyn EJ, Snider RK, Kabara JF, Bonds AB (1997) Stimulus-dependent modulation of spike burst length in cat striate cortical cells. *J Neurophysiol* 78:199-213.
- Dittman JS, Regehr WG (1998) Calcium dependence and recovery kinetics of presynaptic depression at the climbing fiber to Purkinje cell synapse. *J Neurosci* 18:6147-6162.
- Dittman JS, Kreitzer AC, Regehr WG (2000) Interplay between facilitation, depression, and residual calcium at three presynaptic terminals. *J Neurosci* 20:1374-1385.
- Dobrunz LE, Stevens CF (1997) Heterogeneity of release probability, facilitation, and depletion at central synapses. *Neuron* 18:995-1008.
- Dobrunz LE, Stevens CF (1999) Response of hippocampal synapses to natural stimulation patterns. *Neuron* 22:157-166.
- Dobrunz LE, Huang EP, Stevens CF (1997) Very short-term plasticity in hippocampal synapses. *Proc Natl Acad Sci USA* 94:14843-14847.
- Dodge FA Jr, Rahamimoff R (1967) Co-operative action of calcium ions in transmitter release at the neuromuscular junction. *J Physiol* 193:419-432.
- Ekholm A, Hyvärinen J (1970) A pseudo-Markov model for series of neural spike events. *Biophys J* 10:773-796.
- Fano U (1947) Ionization yield of radiations. II. The fluctuations of the number of ions. *Phys Rev* 72:26-29.
- Fisher SA, Fischer TM, Carew TJ (1997) Multiple overlapping processes underlying short-term synaptic enhancement. *Trends Neurosci* 20:170-177.
- Forti L, Bossi M, Bergamaschi A, Villa A, Malgaroli A (1997) Loose-patch recordings of single quanta at individual hippocampal synapses. *Nature* 388:874-878.
- Galarreta M, Hestrin S (1998) Frequency-dependent synaptic depression and the balance of excitation and inhibition in the neocortex. *Nature Neurosci* 1:587-594.
- Goldman MS, Nelson SB, Abbott LF (1999) Decorrelation of spike trains by synaptic depression. *Neurocomputing* 26/27:147-153.
- Gray CM (1999) The temporal correlation hypothesis of visual feature integration: still alive and well. *Neuron* 24:31-47.
- Gray CM, McCormick DA (1996) Chattering cells: superficial pyramidal neurons contributing to the generation of synchronous oscillations in the visual cortex. *Science* 274:109-113.
- Grüneis F, Nakao M, Mizutani Y, Yamamoto M, Meesmann M, Musha T (1993) Further study on $1/f$ fluctuations observed in central single neurons during REM sleep. *Biol Cybern* 68:193-198.
- Hjelmstad GO, Nicoll RA, Malenka RC (1997) Synaptic refractory period provides a measure of probability release in the hippocampus. *Neuron* 19:1309-1318.
- Hsu S-F, Augustine GJ and Jackson MB (1996) Adaptation of Ca^{2+} -triggered exocytosis in presynaptic terminals. *Neuron* 17:501-512.
- Korn H, Faber DS (1987) Regulation and significance of probabilistic release mechanisms at central synapses. In: *Synaptic function* (Edelman GM, Gall WE, Cowan WM, eds), pp. 57-108. New York: John Wiley.
- Korn H, Faber DS (1991) Quantal analysis and synaptic efficacy in the CNS. *Trends Neurosci* 14:439-445.
- Korn H, Sur C, Charpier S, Legendre P, Faber DS (1994) The one-vesicle hypothesis and multivesicular release. In: *Molecular and cellular mechanisms of neurotransmitter release* (Stjärne L, Greengard P, Grillner S, Hökfelt T, Ottoson D, eds), pp. 301-322. New York: Raven Press.
- Kreitzer AC, Regehr WG (2000) Modulation of transmission during trains at a cerebellar synapse. *J Neurosci* 20:1348-1357.
- Kuffler SW, FitzHugh R, Barlow HB (1957) Maintained activity in the cat's retina in light and darkness. *J Gen Physiol* 40:683-702.
- Liley AW, North KAK (1952) An electrical investigation of effects of repetitive stimulation of mammalian neuromuscular junction. *J Neurophysiol* 16:509-527.
- Lisman JE (1997) Bursts as a unit of neural information: making unreliable synapses reliable. *Trends Neurosci* 20:38-43.
- Liu G, Tsien RW (1995) Properties of synaptic transmission at single hippocampal synaptic boutons. *Nature* 375:404-408.
- Liu YH, Wang X-J, Williams GV, Rao S and Goldman-Rakic PS (1998) Analysis of temporal structure of spike trains recorded from monkey prefrontal cortex during working memory tasks. *Soc Neurosci Abstr* 24:1426.
- Livingstone MS, Freeman DC, Hubel DH (1996) Visual responses in V1 of freely viewing monkeys. *Cold Spring Harb Symp Quant Biol* 61:27-37.
- Lowen SB and Teich MC (1991) Doubly stochastic Poisson point process driven by fractal shot noise. *Phys Rev A* 43:4192-4215.
- Lowen SB, Teich MC (1996) The periodogram and Allan variance reveal fractal exponents greater than unity in auditory-nerve spike trains. *J Acoust Soc Am* 99:3585-3591.
- Lowen SB, Cash SS, Poo M-M, Teich MC (1997) Quantal neurotransmitter secretion rate exhibits fractal behavior. *J Neurosci* 17:5666-5677.
- Maass W, Zador AM (1999) Dynamic stochastic synapses as computational units. *Neural Comput* 11:903-917.
- Magleby KL (1987) Short-term changes in synaptic efficacy. In: *Synaptic function* (Edelman G, Gall W, Cowan W, eds), pp. 21-56. New York: Wiley.
- Mandl G (1993) Coding for stimulus velocity by temporal patterning of spike discharges in visual cells of cat superior colliculus. *Vis Res* 33:1451-1475.
- Markram H, Tsodyks M (1996) Redistribution of synaptic efficacy between neocortical pyramidal neurons (Letter). *Nature* 382:807-810.
- Markram H, Wang Y, Tsodyks M (1998) Differential signaling via the same axon of neocortical pyramidal neurons. *Proc Natl Acad Sci USA* 95:5323-5328.
- Matveev V, Wang X-J (2000) Implications of all-or-none synaptic transmission and short-term depression beyond vesicle depletion: a computational study. *J Neurosci* 20:1575-1588.
- Melkonian DS, Kostopoulos GK (1996) Stochastic particle formulation of the vesicle hypothesis. Relevance to short-term phenomena. *NeuroReport* 7:937-942.
- Mueller CG (1954) A quantitative theory of visual excitation for the single photoreceptor. *Proc Natl Acad Sci USA* 40:853-863.
- Murthy VN, Stevens CF (1998) Synaptic vesicles retain their identity through the endocytic cycle. *Nature* 392:497-501.
- Murthy VN, Sejnowski TJ, Stevens CF (1997) Heterogeneous release properties of visualized individual hippocampal synapses. *Neuron* 18:599-612.
- Neher E (1998) Vesicle pools and Ca^{2+} microdomains: new tools for understanding their roles in neurotransmitter release. *Neuron* 20:389-399.
- Neher E, Zucker RS (1993) Multiple calcium-dependent processes related to secretion in bovine chromaffin cells. *Neuron* 10:21-30.
- O'Donovan MJ, Chub N (1997) Population behavior and self-organization in the genesis of spontaneous rhythmic activity by developing spinal networks. *Semin Cell Dev Biol* 8:21-28.

- O'Donovan MJ, Rinzel J (1997) Synaptic depression: a dynamic regulator of synaptic communication with varied functional roles. *Trends Neurosci* 20:431-433.
- Quastel DMJ (1997) The binomial model in fluctuation analysis of quantal neurotransmitter release. *Biophys Journal* 72:728-753.
- Redman SJ (1990) Quantal analysis of synaptic potentials in Neurons of the central nervous system. *Physiol Rev* 70: 165-198.
- Reyes A, Lujan R, Rozov A, Burnashev N, Somogyi P, Sakmann B (1998) Target-cell-specific facilitation and depression in neocortical circuits. *Nature Neurosci* 1:279-285.
- Rosenmund C, Stevens CF (1996) Definition of the readily releasable pool of vesicles at hippocampal synapses. *Neuron* 16:1197-1207.
- Ruderman DL (1994) The statistics of natural images. *Network* 5:517-548.
- Ryan TA, Reuter H, Smith SJ (1997) Optical detection of a quantal presynaptic membrane turnover. *Nature* 388:478-482.
- Schikorski T, Stevens CF (1997) Quantitative ultrastructural analysis of hippocampal excitatory synapses. *J Neurosci* 17:5858-5867.
- Senn W, Wyler K, Streit J, Larkum J, Lüscher H-R, Mey H, Müller L, Steinhauser D, Vogt K, Wannier Th (1996) Dynamics of a random neural network with synaptic depression. *Neural Networks* 9:575-588.
- Singer W (1999) Neuronal synchrony: a versatile code for the definition of relations? *Neuron* 24:49-65.
- Smith DR, Smith GK (1965) A statistical analysis of the continual activity of single cortical neurones in the cat unanaesthetized isolated forebrain. *Biophys J* 5:47-74.
- Somogyi P, Tamas G, Lujan R, Buhl EH (1998) Salient features of synaptic organisation in the cerebral cortex. *Brain Res Rev* 26:113-135.
- Stanley EF (1986) Decline in calcium cooperativity as the basis of facilitation at the squid giant synapse. *J Neurosci* 6:782-789.
- Stevens CF, Tsujimoto T (1995) Estimates for the pool size of releasable quanta at a single central synapse and for the time required to refill the pool. *Proc Natl Acad Sci USA* 92:846-859.
- Stevens CF, Wang Y (1995) Facilitation and depression at single central synapses. *Neuron* 14:795-802.
- Tank DW, Regehr WG, Delaney KR (1995) A quantitative analysis of presynaptic calcium dynamics that contribute to short-term enhancement. *J Neurosci* 15:7940-7952.
- Teich MC (1989) Fractal character of the auditory neural spike train. *IEEE Trans Biomed Engng* 36:150-160.
- Teich MC (1992) Fractal neuronal firing patterns. In: *Single neuron computation* (McKenna T, Davis J, Zornetzer S, eds), pp. 589-625. Boston, MA: Academic Press.
- Teich MC, Heneghan C, Lowen SB, Ozaki T, Kaplan E (1997) Fractal character of the neural spike train in the visual system of the cat. *J Opt Soc Am A* 14:529-546.
- Thomson AM (1997) Activity-dependent properties of synaptic transmission at two classes of connections made by rat neocortical pyramidal axons *in vitro*. *J Physiol* 502:131-147.
- Thomson AM, Deuchars J (1997) Synaptic interactions in neocortical local circuits: dual intracellular recordings *in vitro*. *Cereb Cortex* 7:510-522.
- Thomson AM, West DC, Hahn J, Deuchars J (1996) Single axon IPSPs elicited in pyramidal cells by three classes of interneurons in slices of rat neocortex. *J Physiol* 496:81-102.
- Triller A, Korn H (1982) Transmission at a central inhibitory synapse. III. Ultrastructure of physiologically identified and stained terminals. *J Neurophysiol* 48:708-736.
- Tsodyks MV, Markram H (1997) The neural code between neocortical pyramidal neurons depends on neurotransmitter release probability. *Proc Natl Acad Sci USA*, 94:719-723.
- Turcott RG, Barker PDR, Teich MC (1995) Long-duration correlation in the sequence of action potentials in an insect visual interneuron. *J Statist Comput Simul* 52:253-271.
- Varela JA, Sen K, Gibson J, Fost J, Abbott LF, Nelson SB (1997) A quantitative description of short-term plasticity at excitatory synapses in layer 2/3 of rat primary visual cortex. *J Neurosci* 17:7926-7940.
- Varela JA, Song S, Turrigiano GG, Nelson SB (1999) Differential depression at excitatory and inhibitory synapses in visual cortex. *J Neurosci*, 19:4293-4304.
- Vere-Jones D (1966) Simple stochastic models for the release of quanta of transmitter from a nerve terminal. *Austr J Statist* 8:53-63.
- van Hateren JH (1997) Processing of natural time series of intensities by the visual system of the blowfly. *Vis Res* 37:3407-3416.
- Walmsley B, Alvarez FJ, Fyffe RE (1998) Diversity of structure and function at mammalian central synapses. *Trends Neurosci* 21:81-88.
- Wang X-J (1999) Fast burst firing and short-term synaptic plasticity: a model of neocortical chattering neurons. *Neuroscience* 89:347-362.
- Wise ME (1981) Spike interval distributions for neurons and random walks with drift to a fluctuating threshold. *Statistical distributions in scientific work*, Vol. 6 (Taillie CEA, ed.), pp. 211-231. Boston, MA: Reidel.
- Wu LG, Betz WJ (1998) Kinetics of synaptic depression and vesicle recycling after tetanic stimulation of frog motor nerve terminals. *Biophys J* 74:3003-3009.
- Zucker RS (1989) Short-term synaptic plasticity. *Annu Rev Neurosci* 12:13-31.
- Zucker RS (1996) Exocytosis: a molecular and physiological perspective. *Neuron* 17:1049-1055.